

Self-assembled growth and enhanced blue emission of SiO_xN_y -capped silicon nanowire arrays

T. Qiu and X. L. Wu^{a)}

National Laboratory of Solid State Microstructures and Department of Physics, Nanjing University, Nanjing 210093, People's Republic of China

G. J. Wan,^{b)} Y. F. Mei, G. G. Siu, and Paul K. Chu

Department of Physics and Materials Science, City University of Hong Kong, Kowloon, Hong Kong, People's Republic of China

(Received 29 December 2004; accepted 30 March 2005; published online 5 May 2005)

Unique structured SiO_xN_y -capped Si nanowire arrays were fabricated via electroless metal deposition on α - SiO_xN_y -covered Si wafer in ionic silver HF solution through selective chemical etching. A self-assembled localized microscopic electrochemical cell model and a diffusion-limited aggregation process are associated with the formation of the SiO_xN_y -capped Si nanowire arrays. An enhanced blue photoluminescence band has been recorded. Emission and excitation spectral analyses suggest that generation of photoexcited carriers takes place mainly in the quantum confined Si nanowires, whereas their radiative recombination occurs in the Si–N binding states of SiO_xN_y nanocaps. © 2005 American Institute of Physics. [DOI: 10.1063/1.1929069]

Currently Si nanowires (SiNWs) have attracted considerable attention due to their potential applications in interconnection and basic components for future nanoelectronic and especially optoelectronic devices.^{1,2} Based on the vapor-liquid-solid growth mechanism,³ various techniques have been developed to fabricate the SiNWs.^{4–7} However, these, often complicated, routes typically yield disordered entanglements of nanowires, a fact which hampers their experimental characterization and potential applications. The fabrication of an ordered Si nanowire array, therefore, constitutes an important and challenging issue. Recently, we have reported the ultraviolet (UV) emitting property of Ag-capped SiNWs which can be expected to have favorable applications in optoelectronics such as nanowire UV photodetector.⁸ The UV photoluminescence (PL) is considered to be due to an optical transition in the vacancy defect centers in silver nanocaps on the SiNWs. It is in no way related to SiNWs, since highly efficient photoexcited carriers produced by the quantum confinement on the SiNWs cannot be transferred to the defect states of Ag nanocaps (metal and semiconductor have completely different energy gap structures).^{9,10} In order to attain efficient carrier transfer and at the same time obtain visible emission, a promising technique is to assemble visible light-emitting semiconductor nanomaterials at the tips of SiNWs,^{11,12} reminiscent of nanobeacons, which will be useful in future nanodevices. However, the relevant work has not been reported so far.

In this letter, we present a relatively rapid method of fabricating SiO_xN_y -capped SiNW arrays of enhanced blue emission via electroless metal deposition on a plasma-treated Si wafer in ionic silver HF solution through selective etching. Electroless metal deposition is a simple and inexpensive fabrication technique and has been widely used in microelectronics and in the metal coating industry.^{13,14}

α - SiO_xN_y thin films were deposited on *p*-type, B-doped Si (100) (1–5 Ω cm) wafers using plasma immersion ion implantation and deposition (PIII&D). The details of the PIII&D system have been reported elsewhere.^{15,16} A Si rod was ignited as an arc source by a high pulsed voltage to produce Si plasma. During the deposition, a mixture of nitrogen (15 sccm) and oxygen (3 sccm) was bled into the chamber to maintain a working pressure of 5.0×10^{-4} Torr. The applied voltage was -200 V dc. The deposition time was 90 min. After the deposition, one set of samples were etched in a 5.0 mol/L HF solution containing 0.02 mol/L silver nitrate at 50° C for 10 min, followed by ultrasound treatment in a water bath for 1 min to clean the surface. The container was a conventional Teflon-lined stainless-steel vessel. The Si wafers were then rinsed with deionized water and blown dry in air. The morphology and chemical composition of the samples were examined with a FEG JSM 6335 field-emission scanning electron microscope (SEM) and a PHI 5600 x-ray photoelectron spectrometer (XPS) with monochromatic Al $K\alpha$ source at 14 kV and 350 W. The photoelectron take-off angle was 45°. PL and PL excitation (PLE) measurements were carried out on a Perkin–Elmer LS50B fluorescence spectrophotometer. All of the measurements were taken at room temperature.

Figure 1(a) is a cross-sectional SEM image of α - SiO_xN_y thin film on the Si wafer fabricated using PIII&D. The thickness of SiO_xN_y layer is approximately 150 nm. A large-area SiO_xN_y -capped Si nanowire array could be observed on the surface layer of the Si wafer, which is shown in Figs. 1(b) and 1(c). Figure 1(b) is the cross-sectional SEM image of an oriented SiNW array prepared in a mixed HF–AgNO₃ solution for 10 min and followed by ultrasound treatment in a water bath for 1 min to clean the surface. We can see that the SiNWs are nearly perfectly perpendicular to the surface of the Si wafer and have a uniform distribution. The etched depth (i.e., the lengths of Si nanowires) of the Si wafer is approximately 6 μm . The diameters of nanowires are in the range of 30–200 nm. In Fig. 1(c), one can see tiny silver nanoclusters still attached on the tips of

^{a)} Author to whom correspondence should be addressed; electronic mail: hxxlwu@nju.edu.cn

^{b)} Also affiliated with: College of Materials Science and Engineering, Southwest Jiaotong University.

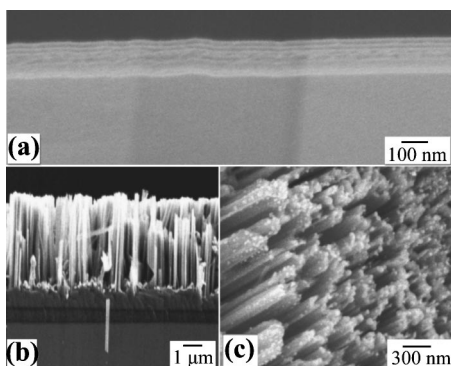


FIG. 1. SEM images of (a) α -SiO_xN_y thin film on the Si wafer, (b) oriented SiO_xN_y-capped SiNWs, and (c) large-area SiO_xN_y-capped SiNWs with tiny silver nanocrystals attached on the tops.

SiO_xN_y-capped SiNWs. Figure 2 shows the XPS spectra of the etched Si wafer with Si 2*p*, N 1*s*, and O 1*s* signals. Three strong XPS signals display direct evidence of the existence of SiO_xN_y caps on the SiNWs.¹⁷ At a depth of around 10 nm, the approximate N and O content is 25% and 30%, respectively.

The formation of the SiO_xN_y-capped Si nanowire arrays can be understood on the basis of self-assembled localized microscopic electrochemical cell model and diffusion-limited aggregation process.^{18,19} Figure 3 gives a schematic diagram of their formation process. At the initial stage, SiO_xN_y-covered Si etching and silver deposition occur simultaneously at the wafer surface. The deposited silver atoms initially form nuclei and then form nanoclusters, uniformly distributed on the surface of the SiO_xN_y-covered Si wafer. These silver nanoclusters and the SiO_xN_y-covered Si areas surrounding these silver nuclei could, respectively, act as local cathodes and anodes in the electrochemical redox reaction process. That is to say, numerous nanometer-sized free-standing electrolytic cells could be spontaneously assembled on the surface of the wafer in aqueous HF solution. Unlike other metal nanoclusters, such as Pt, Cu, Fe, etc. which have a strong tendency to coalesce and form a continuous grain film in the process of electroless metal deposition, silver nanoclusters deposit on the wafer surface to form dendrites, involved in cluster formation by the adhesion of a particle with random path to a selected seed on contact and allowing the particle to diffuse and stick to the formed structure. *In situ* prepared SiNWs around the silver nanoclusters could be regarded as a template of the sort reported by Xiao *et al.*²⁰ in relation to palladium and silver nanostructures. With the progress of silver deposition, silver nanoclusters acting as the

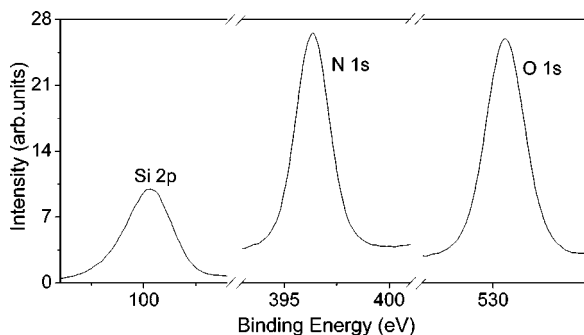


FIG. 2. XPS spectra of Si 2*p*, N 1*s*, and O 1*s*, taken at the sputtered depth of 10 nm of the SiO_xN_y-capped Si nanowire array.

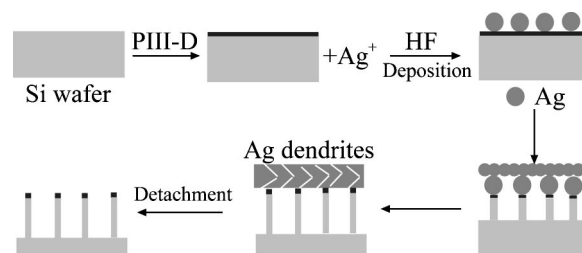


FIG. 3. Schematic illustration of the growth process of the SiO_xN_y-capped Si nanowire array.

cathodes are successfully preserved [Fig. 1(c)], while the surrounding SiO_xN_y-covered Si acting as the anodes is etched away. The presence of these nanoscale electrolytic cells thus leads to selective etching of the SiO_xN_y-covered Si substrate. As a result, the SiO_xN_y-capped SiNW array is formed.

The PL spectrum of the α -SiO_xN_y thin film on the Si wafer, taken under excitation with the 360 nm line of a Xe lamp, is presented in Fig. 4(a). It can be seen that a broad PL peak appears at 520 nm. In addition, the weak existence of a blue PL shoulder is evident at \sim 440 nm (2.8 eV). The PLE spectra of the 520 nm PL, taken by monitoring at 500, 520, and 540 nm, are shown in Fig. 4(b). One can see that with increasing the monitored emission wavelength, the PLE band widens and redshifts. In view of the PLE character, we can attribute the 520 nm PL to optical transition in the tail states of α -SiO_xN_y film.^{11,21} Noma *et al.*²² have experimentally suggested that the 440 nm PL in Si oxynitride has an origin related to Si–N bonds. Theoretical calculations by Ance *et al.*²³ pointed out that Si–N bonds can introduce localized states to SiO₂ structure due to N 2*p* lone pair electrons above the O 2*p* lone pair states at the top of the valence band. These localized states are active in hole trapping and transport. Moreover, the top of the valence band is formed by N 2*p* lone pair states in SiO_xN_y with a high Si–N concentration. These theoretical and experimental results support the association of the 440 nm PL with the recombination of holes and electrons in localized states corresponding to Si–N bonds.

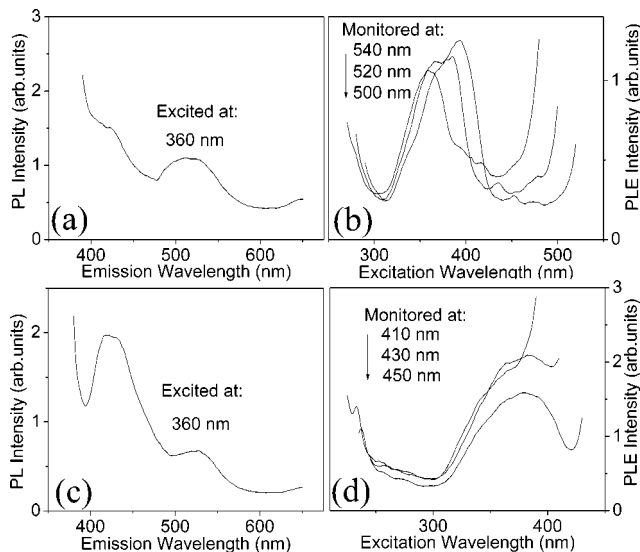


FIG. 4. (a) and (b) PL and PLE spectra of α -SiO_xN_y thin film. (c) and (d) PL and PLE spectra of SiO_xN_y-capped Si nanowire array.

Figure 4(c) shows the PL spectrum of a SiO_xN_y -capped Si nanowire array, taken under excitation with the 360 nm line of a Xe lamp. One can see that the two PL peaks at 440 and 520 nm still exist. Obviously, the 440 nm PL is greatly enhanced compared to that in Fig. 4(a). To identify the origin of the enhanced 440 nm PL, we examined the PLE spectra by monitoring at different emission wavelengths around 440 nm. The corresponding result is presented in Fig. 4(d). We can see that the three PLE spectra all contain a broad PLE band at 380 nm. The broad PLE band is inherent in all systems containing Si nanocrystals, and has been shown to originate from a band-to-band excitation process with a quantum confinement feature.^{9,10} Thus, we can infer that the photoexcited carriers for the enhanced 440 nm radiation mainly originate in the quantum confined SiNWs with smaller sizes, while their radiative recombination occurs in the Si–N bonding states of SiO_xN_y nanocaps on the tops of the SiNWs.

In summary, a rapid inexpensive method of fabricating a SiO_xN_y -capped SiNW array has been described on the basis of electroless metal deposition technique. The formation of the SiO_xN_y -capped SiNW array can be interpreted on the basis of self-assembled localized microscopic electrochemical cell model and diffusion-limited aggregation process. An enhanced blue PL band is observed at 440 nm. The PL and PLE spectral analyses strongly suggest that generation of photoexcited carriers takes place in the quantum confined SiNWs, while their radiative recombination occurs at Si–N bonds of SiO_xN_y nanocaps.

This work was supported by a grant (No. 10225416) from the Natural Science Foundation of China and by Hong Kong Research Grants Council (RGC) Competitive Earmarked Research Grants (CERG) Nos. CityU 1137/03E and CityU 1120/04E, and City University of Hong Kong Strategic Research Grant (SRG) No. 7001642.

- ¹Y. Cui and C. M. Lieber, *Science* **291**, 851 (2001).
- ²Y. Cui, Q. Q. Wei, H. K. Park, and C. M. Lieber, *Science* **293**, 1289 (2001).
- ³R. S. Wagner and W. C. Ellis, *Appl. Phys. Lett.* **4**, 89 (1964).
- ⁴T. I. Kamins, R. S. Williams, Y. Chen, Y. L. Chang, and Y. A. Chang, *Appl. Phys. Lett.* **76**, 562 (2000).
- ⁵A. M. Morales and C. M. Lieber, *Science* **279**, 208 (1998).
- ⁶G. C. Xiong, H. T. Zhou, and S. O. Feng, *Appl. Phys. Lett.* **72**, 3458 (1998).
- ⁷J. D. Holmes, K. P. Johnston, R. C. Doty, and B. A. Korgel, *Science* **287**, 1471 (2000).
- ⁸T. Qiu, X. L. Wu, X. Yang, G. S. Huang, and Z. Y. Zhang, *Appl. Phys. Lett.* **84**, 3867 (2004).
- ⁹Y. H. Xie, W. L. Wilson, F. M. Ross, J. A. Mucha, E. A. Fitzgerald, J. M. Macaulay, and T. D. Harris, *J. Appl. Phys.* **71**, 2403 (1992).
- ¹⁰X. L. Wu, S. J. Xiong, D. L. Fan, Y. Gu, and X. M. Bao, *Phys. Rev. B* **62**, R7759 (2000).
- ¹¹B. H. Augustine, Y. Z. Hu, E. A. Irene, and L. E. McNeil, *Appl. Phys. Lett.* **67**, 3694 (1995).
- ¹²B. H. Augustine, E. A. Irene, Y. J. He, K. J. Price, L. E. McNeil, K. N. Christensen, and D. M. Maher, *J. Appl. Phys.* **78**, 4020 (1995).
- ¹³R. Sard, Y. Okinaka, and H. A. Waggenger, *J. Electrochem. Soc.* **136**, 462 (1989).
- ¹⁴D. B. Wolfe, J. C. Love, K. E. Paul, M. L. Chabiny, and G. M. Whitesides, *Appl. Phys. Lett.* **80**, 2222 (2002).
- ¹⁵P. K. Chu, B. Y. Tang, Y. C. Cheng, and P. K. Ko, *Rev. Sci. Instrum.* **68**, 1866 (1997).
- ¹⁶P. K. Chu, *Surf. Coat. Technol.* **156**, 244 (2002).
- ¹⁷J. F. Moulder, W. F. Stickle, P. E. Sobol, and K. D. Bomben, *Handbook of X-Ray Photoelectron Spectroscopy* (Perkin–Elmer PHI, Eden Prairie, MN, 1992).
- ¹⁸K. Q. Peng, Y. J. Yan, S. P. Gao, and J. Zhu, *Adv. Funct. Mater.* **13**, 127 (2003).
- ¹⁹T. A. Witten, Jr. and L. M. Sander, *Phys. Rev. Lett.* **47**, 1400 (1981).
- ²⁰J. P. Xiao, Y. Xie, R. Tang, M. Chen, and X. B. Tian, *Adv. Mater. (Weinheim, Ger.)* **13**, 1887 (2001).
- ²¹K. J. Price, L. E. McNeil, A. Suvkanov, E. A. Irene, P. J. MacFarlane, and M. E. Zvanut, *J. Appl. Phys.* **86**, 2628 (1999).
- ²²T. Noma, K. S. Seol, H. Kato, M. Fujimaki, and Y. Ohki, *Appl. Phys. Lett.* **79**, 1995 (2001).
- ²³C. Ance, F. D. Chelle, J. P. Ferraton, G. Leveque, P. Ordejon, and F. Yndurain, *Appl. Phys. Lett.* **60**, 1399 (1992).